



CrossMark  
click for updates

Cite this: *RSC Adv.*, 2016, 6, 97832

# Impedimetric detection of pathogenic bacteria with bacteriophages using gold nanorod deposited graphite electrodes†

Farzaneh Moghtader,<sup>ab</sup> Gulsah Congur,<sup>c</sup> Hadi M. Zareie,<sup>de</sup> Arzum Erdem<sup>\*c</sup> and Erhan Piskin<sup>\*ab</sup>

Electrochemical impedance spectroscopy (EIS) is applied for the detection of bacteria using bacteriophages as a bioprobe together with gold nanorods (GNRs). *Escherichia coli* – *E. coli* K12 was used as a model target bacteria and also for the propagation of its specific T4-phages. Gold nanorods (GNRs) were synthesized *via* a two-step protocol and characterized using different techniques. EIS measurements were conducted in an electrochemical cell consisting of a three electrode system. Single-use pencil graphite electrodes (PGE) were modified by the physical adsorption of GNRs to increase their interfacial conductivity and therefore sensitivity for impedimetric measurements. Therefore, interfacial charge-transfer resistance values ( $R_{ct}$ ) sharply decreased after GNRs deposition. Phages were adsorbed on these electrodes *via* a simple incubation protocol at room temperature, which resulted in an increase in  $R_{ct}$  values, which was concluded to be as a result of nonconductive phage layers. These phage-carrying GNRs–PGEs were used for impedimetric detection of the target bacteria, *E. coli*. Significant increases at the  $R_{ct}$  values were observed which were attributed to the insulation effects of the adsorbed bacterial layers. This increase was even more when the bacterial concentrations were higher. In the case of the non-target bacteria *Staphylococcus aureus* (*S. aureus*), conductivity noticeable decreases (due to nonspecific adsorption). However, in the case of *E. coli*, the  $R_{ct}$  value increase is time dependent and reaches maximum in about 25–30 min, then decreases gradually as a result of bacterial lysis due to phage invasion on the electrode surfaces. In contrast, there were no time dependent changes with the non-target bacteria *S. aureus* (no infection and no lytic activity). It is concluded that the target bacteria could be detected using this very simple and inexpensive detection protocol with a minimum detection limit of  $10^3$  CFU mL<sup>-1</sup> in approximately 100  $\mu$ L bacterial suspension.

Received 25th July 2016  
Accepted 28th September 2016

DOI: 10.1039/c6ra18884b

[www.rsc.org/advances](http://www.rsc.org/advances)

## Introduction

According to the WHO (World Health Organization), more than 2.2 million deaths occur annually due to food and water-borne diseases, which are mostly caused by pathogenic bacteria, including *Escherichia coli*, *Salmonella*, *Staphylococcus*, and many others, even in developed countries. The infectious dose of

these pathogens can be very low (around 10 bacteria). The emergence of drug-resistant strains makes this problem very severe. The scenario that we see today is only modern daily life incidences. Highly pathogenic bacteria can also be used as biological warfare agents, and not only are they very common, but they can be easily distributed *via* food and water, and unfortunately living creatures, such as human and animals, as a result of the very intense mobility traffic worldwide. Monitoring food and water quality has therefore been argued as the most important priority towards national and international health and safety issues, with global emphasis on the rapid and early detection of pathogen contamination, especially in food and water.

The current pathogen detection methods include: (i) microbiological techniques (conventional culturing); (ii) nucleic-acid based (*e.g.* PCR and DNA hybridization using oligonucleotides as bio-recognition elements or bio-probes)<sup>1–4</sup> and (iii) immunological (*e.g.*, ELISA using specific antibodies as bio-probes).<sup>5</sup> Microbiological techniques are the oldest, but are still considered the most accurate approach. In this technique,

<sup>a</sup>Hacettepe University, Faculty of Engineering, Chemical Engineering Department, Graduate School of Science and Engineering – Nanotechnology and Nanomedicine Division, 06800, Ankara, Turkey

<sup>b</sup>Biyomedtek/NanoBMT, 06800, Ankara, Turkey. E-mail: [erhanpiskin@biyomedtek.com](mailto:erhanpiskin@biyomedtek.com)

<sup>c</sup>Ege University, Faculty of Pharmacy, Analytical Chemistry Department, 35100, İzmir, Turkey. E-mail: [arzum.erdem@ege.edu.tr](mailto:arzum.erdem@ege.edu.tr); [arzume@hotmail.com](mailto:arzume@hotmail.com)

<sup>d</sup>İzmir Institute of Technology, Department of Material Science and Engineering, 35430, Urla, İzmir, Turkey

<sup>e</sup>University of Technology, School of Physics and Advanced Materials, Microstructural Analysis Unit, Sydney, Ultimo NSW 2007, Australia

† Electronic supplementary information (ESI) available. See DOI: 10.1039/c6ra18884b

the target bacteria are grown in defined culture media, followed by counting the number of colonies, and specific biochemical tests are also applied for more accurate testing. These tests usually take a minimum of a few days or even much longer (few weeks) which is time-consuming and laborious. The more modern/molecular based approaches, such as immunological or nucleic acid-based techniques, typically take a few hours to complete. However, highly experienced experts are needed, sample preparation is time consuming, expensive and highly developed infrastructure is required. Oligonucleotides have been used as bioprobes in which detection is based on the interaction of two complementary oligos (probe and target). There are already commercial products based on nucleic acid (as bioprobes) sensor technology for pathogen detection, however they still have several significant limitations. The purity of the probe-nucleic acid produced by PCR-based amplification methods may not high enough which results false positive findings. The nucleic acids may be degraded which results in false negative indications. It is not possible to observe the viability of the bacteria and it cannot be applied for the detection of bacterial toxins, which are important limitations. These bioprobes exhibit quite high specific affinity towards their target, and several detection systems have been developed for the detection of bacteria, mostly in clinical samples, however they also exhibit quite significant drawbacks which are as follows: (i) antibodies are proteins and are therefore sensitive to temperature, pH, and several chemical and enzymatic attacks and lose their 3D active forms irreversibly; (ii) they are temperature sensitive and therefore should be kept in the refrigerator and should be transported in cold-chain. Also, their shelf life may be short which limits their application; (iii) polyclonal antibodies have several recognition epitopes. They are inexpensive but are not very specific as monoclonal antibodies, therefore care should be taken to not use polyclonal antibodies; and (iv) antibody production is difficult since animals are needed which also brings ethical issues. There are several extensive and good reviews about immuno-based sensors, which also explain their advantages and limitations.

The use of bacteriophages as bio-probes, as an alternative to antibodies and nucleic acids, for bacterial detection is a very unique approach that has been proposed rather recently.<sup>6–8</sup> Bacteriophages are viruses which only infect bacteria, with excellent host selectivity. Bacteriophages are not only the most abundant biological entities but are also probably also the most diverse. They may be very specific even at serotype levels, and could be easily propagated and therefore quite inexpensive and have a long-shelf life. As nicely reviewed recently by Singh *et al.*,<sup>8</sup> bacteriophages have been used for the specific detection of target bacteria using different bio-sensing platforms which are mainly treated in two categories: (i) the use of labels (fluorescent, luminescent, enzymes, electrochemically active labels, *etc.*) and (ii) label-free systems (QCM, SPR, ellipsometer, Raman and mass spectrometry, *etc.*). Almost all of the technologies mentioned above have been applied for the detection of pathogens using bacteriophages with different extents and success. The challenging objective is to develop enhanced detection

technologies with high levels of reliability, sensitivity, and selectivity with short assay times.

Electrochemical biosensors detect targets quite rapidly and sensitively/selectively in comparison to conventional techniques.<sup>9–13</sup> EIS is a powerful electrochemical technique that is capable of detecting small changes occurring at the solution–electrode interface usually without using any reagent.<sup>14,15</sup> EIS for pathogen detection is usually performed either by monitoring the changes in the medium conductivity, which is caused by bacterial growth/metabolism, or the changes in the solution–electrode interface due to microorganism non-specific adsorption or specific capture onto the sensor surface.<sup>16–24</sup>

In recent years due to the size and shape-dependent properties of metallic, especially gold and silver, nanoparticles have been extensively studied in a wide variety of applications, such as photonics, information storage, electronic and optical detection systems, therapeutics, diagnostics, photovoltaics, and catalysis. Especially the following make them excellent materials for bio-based applications: (i) they are easily produced in many different shapes (nanospheres, nanorods, nanocages, nanocubes, *etc.*) and sizes even down to a few nm; (ii) excellent and variable optical (plasmonic) properties; (iii) small sizes, which mean high surface areas; and (iv) easy surface modification/functionalization for bio-probe immobilization, *etc.*<sup>25</sup> Gold nanorods (GNRs) are rod-shape nanoparticles that could easily be produced with different aspect ratios (dimensions) and therefore different plasmonic properties.<sup>26,27</sup> Due to their shapes, less agglomeration at the immobilized surface is usually achieved. Additionally, their unique optical and physical properties have allowed them to be used for the development of bio-sensing platforms.<sup>13,28–32</sup>

Herein, we attempt to use EIS for the selective/rapid/inexpensive detection of pathogenic bacteria using bacteriophages (T4) as bioprobes together with GNRs, which were produced by us with selected dimensions and also successfully applied in our previous electrochemical DNA sensor studies.<sup>13,25</sup>

## Materials and methods

### Apparatus and chemicals

Electrochemical impedance spectroscopy (EIS) measurements were conducted in a Faraday cage (Eco Chemie, The Netherlands) using an IVIUM CompactStat.e with the IVIUM software 2.10 (IVIUM, The Netherlands). The electrochemical cell consisted of a three electrode system with a pencil graphite electrode (PGE, Tombow 0.5, HB), an Ag/AgCl/3 M KCl reference electrode and a platinum wire as the auxiliary electrode (SM-Fig. 1†). Nyquist diagrams were obtained (in less than 10 min) and  $R_{ct}$  values were calculated using the fitting program of the IVIUM software 2.10.<sup>13</sup>

A Tombow pencil was used to hold the graphite leads. A metallic wire was used to solder the metallic part of the pencil in order to provide electrical contact. The graphite leads of 10 mm were immersed for dip-coating as well as all the immobilization steps. 14 mm of the lead extruded outside the pencil and was held with the pencil.

Hexadecyltrimethyl ammonium bromide (CTAB > 99%), tetrachloroauric acid ( $\text{HAuCl}_4 \cdot 3\text{H}_2\text{O}$ ) and sodium borohydride ( $\text{NaBH}_4$ , 99%) were purchased from Sigma-Aldrich (Germany). Silver nitrate ( $\text{AgNO}_3$ , 99.8%) was purchased from Fluka (USA). All other chemicals were purchased from Sigma and Merck. Ultrapure distilled water was used for the preparation of all solutions.

### Gold nanorods and deposition onto PGEs

Gold nanorods (GNRs) were produced by a rather classical two-step process, as also described in the related literature including ours, which is briefly as follows:<sup>13,25</sup> in the first step, in order to synthesize gold spherical nanoparticles, 7.5 mL of a 100 mM aqueous solution of CTAB was sonicated for 20 min at 40 °C in a water bath. Then 250  $\mu\text{L}$  of a 10 mM  $\text{HAuCl}_4 \cdot 3\text{H}_2\text{O}$  aqueous solution was added with continuous stirring under nitrogen atmosphere. Next, 600  $\mu\text{L}$  of a 10 mM ice-cold aqueous solution of  $\text{NaBH}_4$  was added under vigorous stirring in 1 min. The CTAB-capped nanospheres formed were used as seeds within 2–5 h for preparation of GNRs in the next step. 40 mL of the growth solution consisting of CTAB (100 mM) and  $\text{HAuCl}_4 \cdot 3\text{H}_2\text{O}$  (10 mM) was prepared which was dark-yellow. 250  $\mu\text{L}$  of a 10 mM  $\text{AgNO}_3$  aqueous solution and then 270  $\mu\text{L}$  of 100 mM ascorbic acid, which is a mild reducing agent (Sigma-Aldrich, USA), were added to the growth solution flask which resulted in a colorless solution. Then, 210  $\mu\text{L}$  of the CTAB-capped seed solution that was produced in the previous step was added to that flask, and the mixture was gently mixed. After 3 h at 24 °C, the color of the mixture turned dark-blue with a brownish opalescence which was an indication of the formation of GNRs. This nanoemulsion carrying the GNRs was concentrated by centrifugation twice at 6000g for 30 min in order to remove the excess unbound CTAB. The nanoemulsions were characterized via UV-vis spectroscopy (V-530, Jasco, USA) and transmission electron microscopy (TEM) (Tecnai G2 F30, FEI Company, USA) and then were stored at 4 °C until use in the detection studies described below.

The GNRs were deposited onto PGEs with a very simple incubation protocol.<sup>13,25</sup> Briefly, the GNRs nanoemulsions were diluted at different ratios using 50 mM phosphate buffer containing 0.5 mM NaCl (PBS, pH 7.4). The leads were immersed into vials containing 100  $\mu\text{L}$  of 1 : 10, 1 : 20, 1 : 30 and 1 : 40 GNRs : PBS diluted nanoemulsion for 1 h (SM-Fig. 2†). Then, the electrodes were gently rinsed in PBS (pH 7.4) to remove possible contaminants from the medium, such as salts, and freshly used in the EIS measurements.

### Preparation of bacteria/bacteriophages

*Escherichia coli* (*E. coli*), which is a Gram-negative bacterium, was selected as the target and also for the propagation of its specific bacteriophages (T4). *E. coli* K12 and T4 phages were obtained from ATCC (11303 and 11303-B4, respectively). The Luria-Bertani (LB) liquid medium was prepared by dissolving 25 g of LB powder in 1 L of distilled water and this non-pathogenic strain was cultured in the LB medium at 37 °C in a rotary shaker (200 rpm) until it reached the exponential growth phase (about OD 600

nm), which was followed spectrophotometrically for up to 24 h. These bacterial cultures were centrifuged at around 6000 rpm for about 5 min. The pellets obtained were washed a few times and re-suspended in PBS (140 mM NaCl, 2.7 mM KCl, 0.1 mM  $\text{Na}_2\text{HPO}_4$  and 1.8 mM  $\text{KH}_2\text{PO}_4$ , pH: 7.2). Different concentrations of this suspension were prepared by dilution and then they were plated in LB agar which was prepared by adding 6 g of granulated agar to 400 mL of LB media to estimate the total bacterial (viable) counts (color forming units, CFU). Bacterial suspensions containing the Gram positive bacteria *Staphylococcus aureus* were also prepared to use as the non-target bacteria.

T4 phages were amplified using the bacterial suspension prepared in the previous step as follows:<sup>33,34</sup> 100  $\mu\text{L}$  of  $10^6$  CFU  $\text{mL}^{-1}$  *E. coli* K12 and 100  $\mu\text{L}$  of  $10^6$  PFU  $\text{mL}^{-1}$  T4 phage were mixed in a test tube using a vortex mixer. The mixture was incubated at room temperature for 15 min and then added to a 20 mL tube containing LB media. The mixture was incubated for 6 h at 37 °C in a shaking incubator (200 rpm). 10% (v/v) chloroform was finally added and the solution was kept at 4 °C for 20 min. For purification, the medium was first ultra-filtered through a sterile 0.2  $\mu\text{m}$  filter and then centrifuged at 4 °C (12 000g). The purified phages were re-suspended in sterile PBS, and the phage concentration (plaque forming unit per mL (PFU  $\text{mL}^{-1}$ )) was determined as follows: serial decimal phage dilutions were prepared from the initial phage suspension, where 100  $\mu\text{L}$  from each suspension and 400  $\mu\text{L}$  of *E. coli* suspension were added to a semi-liquid medium LB (agar 7.5 g  $\text{L}^{-1}$ ). The mixture was suddenly added on a solid medium and incubated at 37 °C for 24 h. A titration was performed by direct counting of the lysis plaques. The phage stock produced in this way was about  $10^6$  PFU  $\text{mL}^{-1}$ , which was stored at 4 °C and used after proper dilutions.

The effectiveness, which is the infection and destruction of the bacteria (*E. coli* here), of the T4 phages propagated in the previous steps was evaluated by a culture method. Plates containing agar broth with the target bacteria *E. coli* were prepared. The phages were placed on the agar in the plates which were then incubated at 37 °C overnight. Note that the developing *E. coli* lawn plates were originally turbid. However, *E. coli* was destroyed by the phages and transparent zones were formed due to lysis of the bacteria which were measured to determine the effectiveness of the phages. The specificity of the phages was demonstrated by using them in the non-target (*S. aureus*) cultures parallel to the *E. coli* culture tests.

### Scanning electron microscopy (SEM) imaging

SEM micrographs of the support (pencils) and the GNRs, phages and target bacteria on the graphite pencil surfaces were obtained using a Philips Ultra Plus High Resolution FESEM (The Netherlands) equipped with an in-lens secondary-electron detector operating in the range of 2–20 keV, depending on sample charging.

### Electrochemical detection

All EIS measurements were performed in the presence of a 2.5 mM  $\text{K}_3[\text{Fe}(\text{CN})_6]/\text{K}_4[\text{Fe}(\text{CN})_6]$  (1 : 1) mixture as a redox probe

prepared in 0.1 M KCl. Impedance spectra were obtained in the frequency range of 100 mHz to 100 kHz in a potential of 0.23 V versus Ag/AgCl/3 M KCl with a voltage amplitude of 10 mV. The respective semicircle diameter corresponds to the charge-transfer resistance,  $R_{ct}$ , calculated after fitting by Randles circuit, which is comprised of solution resistance ( $R_s$ ), space charge capacitance at the electrode/electrolyte interface ( $Q$ ), Warburg impedance ( $W$ ) and  $R_{ct}$ .<sup>13,35</sup> The frequency interval was divided into 97 logarithmically equidistant measure points.

Firstly, EIS spectra of the freshly prepared GNRs-PGEs were obtained. Then, the GNRs deposited PGEs were immersed into vials containing the T4-phage suspensions (100  $\mu$ L of the stock solution with  $10^6$  PFU  $\text{mL}^{-1}$  and 1 : 2, 1 : 5, 1 : 10 phage : PBS diluted solutions) and incubated at room temperature for 1 h, followed by washing with PBS (pH 7.4), and then were used in the EIS measurements.

The T4-phage immobilized GNRs-PGEs were incubated with 100  $\mu$ L of *E. coli* K12 suspensions ( $10^2$  to  $10^6$  CFU  $\text{mL}^{-1}$ ) at room temperature for different incubation times ranging from 10 to 60 min. The electrodes were rinsed with PBS (pH 7.4) to avoid nonspecific adsorptions. In order to test selectivity, the GNRs-PGEs carrying T4 phages were also interacted with 100  $\mu$ L of *S. aureus* suspensions ( $10^4$  CFU  $\text{mL}^{-1}$ ) at the same conditions given above.

## Results and discussion

In this study, GNRs were produced by a rather classical two-step process; (i) gold nanospheres were synthesized and (ii) used as seeds for one dimensional growth to form nanorods as reported previously.<sup>25</sup> The average sizes of the GNRs were  $32.8 \pm 1.8$  nm (length) and  $6.7 \pm 1.2$  nm (width/diameter) according to TEM analysis and estimation from a classical software (ImageJ). Stabilization of the GNRs was achieved using CTAB.<sup>36,37</sup> The

recommended aspect ratio of the GNRs was achieved as 4.8 by using a CTAB/HAuCl<sub>4</sub> molar ratio more than 10.<sup>38,39</sup> We studied the effects of almost all experimental parameters on the gold nanorod size and stability in our previous work related to electrochemical DNA biosensors.<sup>25</sup>

UV-vis spectrophotometry was utilized to analyze the GNRs formation and their plasmonic properties (Fig. 1). The GNRs gave two peaks according to their two dimensional structure. It should be noted that the peak locations also reflect roughly the aspect ratios of the nanorods, since only a single peak is observed for nanospheres.

The representative SEM micrographs given in Fig. 2 explain in detail the steps of the detection protocol applied in this study. The graphite electrode surfaces ("PGEs") are quite rough and simple dipping (incubation) is enough to physically deposit the GNRs on their surfaces, (Fig. 2A and B, respectively). In the second step the PGEs carrying GNRs were incubated within the phage emulsions (stoke) and it is noticed that there are a few nanorods around, and most probably many others are under the phage layers (Fig. 2C). The phage-loaded electrodes were then immersed into the bacterial suspensions for impedimetric detection. Very unusual/interesting SEM images are given in Fig. 2D to demonstrate of what occurred on the electrode surfaces. A significant number of black silhouettes (shadow) from the target bacteria *E. coli* are observed, which were invaded/destroyed by the phages and desorbed from the surfaces. This is also indicated in the impedimetric analysis described below. Fig. 2E demonstrates even very interesting behavior. It seems that some of the physically adsorbed – positively charged GNRs are detach from the graphite surfaces and accumulate onto the negatively charge bacterial walls, and interestingly prevents destruction of those bacteria by phages and also release from the surfaces of the graphite.

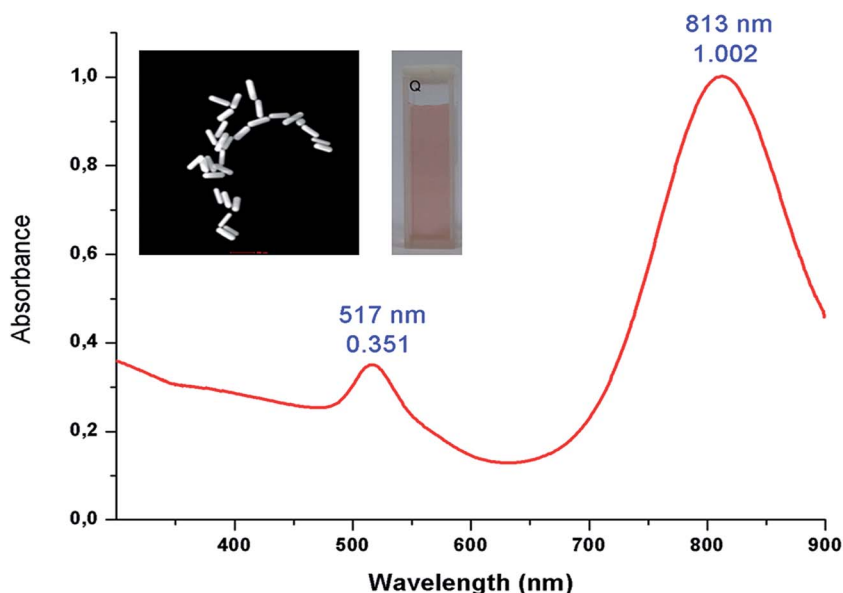


Fig. 1 Representative UV-vis spectrum of the AuNRs nanoemulsion. A typical TEM image and a picture of the nanoemulsion are also presented in the inset (left-top).

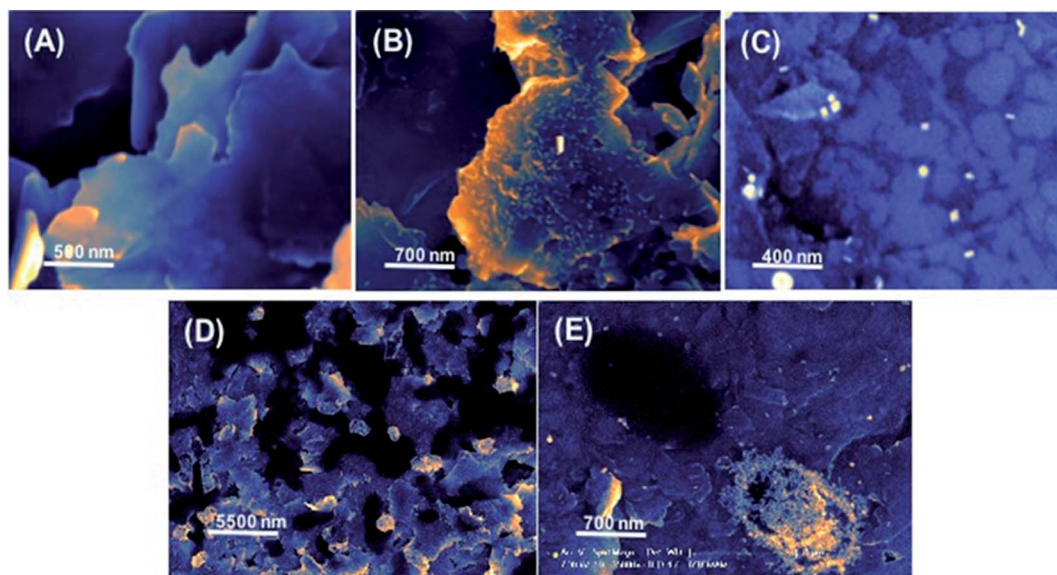


Fig. 2 SEM micrographs of the detection protocol of bacteria and bacteriophages. (A) Pure pencil graphite, (B) after treatment with GNRs, (C) bacteriophages with GNRs, and (D and E) low and high magnification of the GNRs, bacteria and bacteriophages together.

Impedimetric measurements with the PGEs and their GNRs loaded forms were conducted, in which the average  $R_{ct}$  was obtained as  $199.2 \pm 33.8 \Omega$  (relative standard deviation (RSD)% = 17.0%,  $n = 6$ ) for the unmodified PGEs (Fig. 3A and Table 1A). After the deposition of GNRs onto the PGE surfaces the  $R_{ct}$  values sharply decreased which is the result of enhanced electron transfer due to the excellent conductive properties of the gold nanoparticles with high surface areas.<sup>11,13,40</sup> The highest conductivity increase and reproducible  $R_{ct}$  values were observed for the surfaces prepared with a 1 : 10 dilution (Fig. 3B and Table 1B). The average  $R_{ct}$  measured was  $26.2 \pm 3.4 \Omega$  with an RSD% of 13.1% ( $n = 6$ ) and the decrease ratio was 86.9%.

Immobilization of the bioprobe bacteriophages onto the GNRs-PGE was achieved by simple adsorption from the T4-phages nanoemulsion ( $100 \mu\text{L}$ ,  $10^6 \text{ PFU mL}^{-1}$ ) and its diluted forms at room temperature (Fig. 4). The  $R_{ct}$  was calculated to be  $340.5 \pm 35.6 \Omega$  after the immobilization of the stock solution of bacteriophage at the surface of the GNRs-PGE (Fig. 4C and Table 1C) which resulted in an almost 12 fold increase in  $R_{ct}$  value in comparison to that obtained by the AuNR-PGEs (Fig. 4B and Table 1B). This increase in  $R_{ct}$  may be attributed to the insulation effect of the phage layers onto the surfaces of the electrodes.<sup>22,34</sup> The highest and most reproducible  $R_{ct}$  was obtained by using the stock solution of the bacteriophage, thus it was used for immobilization at the surface of the GNRs-PGEs without any dilution.

The interaction of the target bacteria *E. coli* K12 and its bacteriophage for 1 h was then studied using the GNRs-PGEs. The average  $R_{ct}$  value obtained was  $378.2 \pm 51.4 \Omega$  after the interaction with *E. coli* K12 at  $10^2 \text{ CFU mL}^{-1}$ . This result shows that our impedimetric biosensor could detect *E. coli* K12 even at a concentration level of  $10^2 \text{ CFU mL}^{-1}$ . It was clearly seen that the  $R_{ct}$  increased when the *E. coli* K12 concentration increased.<sup>22,24,34,41</sup> The same experiment was also performed in

the presence of *S. aureus* and the differences between the  $R_{ct}$  values obtained in the presence of *E. coli* K12 and *S. aureus* at concentrations from  $10^2$  to  $10^6 \text{ CFU mL}^{-1}$  were calculated. As seen in Table 2, the difference in the  $R_{ct}$  values for the target (*E. coli*) and non-target (*S. aureus*) was not significantly different. It should be noted that we have bacteriophages specific to *E. coli*, therefore we were expecting very significant differences for the target and non-target adsorption onto the pencil electrode surfaces in order to exhibit the specificity of our approach. However, this did not occur, which was rather frustrating. Therefore, we decided not to use the data in Table 2 for the preparation of the calibration curve of the EIS biosensor and

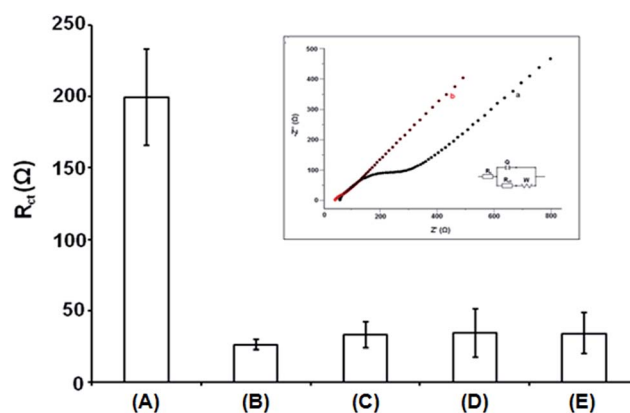
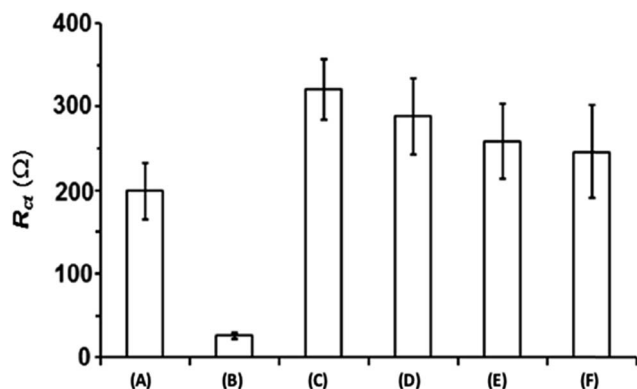


Fig. 3 Histograms representing the  $R_{ct}$  values obtained using: (A) the unmodified PGE; and (B–E) the PGEs after GNRs deposition from the nanorod-emulsions diluted 1/10; 1/20; 1/30 and 1/40 times. Three repetitive measurements were done in each experimental group. A representative Nyquist diagram representing (A) the unmodified PGE, and (B) the 1/10 diluted GNRs deposited PGE obtained using EIS is given in the inset, and the equivalent circuit model used to fit the impedance data.

**Table 1**  $R_{ct}$  values obtained using EIS with (A) the unmodified PGEs, (B) the GNRs deposited PGEs, and (C) the T4 phage immobilized PGEs ( $100 \mu\text{L}$ ,  $10^6$  PFU  $\text{mL}^{-1}$ ) at room temperature for 1 h

	(A)	(B)	(C)
$R_{ct}$ ( $\Omega$ )	$199.2 \pm 33.8$	$26.2 \pm 3.4$	$340.5 \pm 35.6$



**Fig. 4** Histograms representing the  $R_{ct}$  values obtained using: (A) the unmodified PGEs; (B) the GNRs deposited PGEs; and after incubation of the GNRs-PGEs in (C) the stock solution of the T4-phages ( $100 \mu\text{L}$ ,  $10^6$  PFU  $\text{mL}^{-1}$ ), and in (D–F) the T4-phage nanoemulsions ( $100 \mu\text{L}$ ,  $10^6$  PFU  $\text{mL}^{-1}$ ) after dilution 1 : 2, 1 : 5 and 1 : 10 times, respectively, for 1 h at room temperature.

**Table 2**  $R_{ct}$  ( $\Omega$ ) and  $\Delta R_{ct}$  ( $\Omega$ ) values representing the difference between the  $R_{ct}$  values obtained from *E. coli* K12 and *S. aureus* – after interaction with T4 phages and *E. coli* K12 and *S. aureus* using the GNRs-PGEs at room temperature for 1 h

Concentration (CFU $\text{mL}^{-1}$ )	$R_{ct}$ ( $\Omega$ )		$\Delta R_{ct}$ ( $\Omega$ )
	<i>E. coli</i> K12	<i>S. aureus</i>	
$10^2$	$378.2 \pm 51.4$	$360.5 \pm 45.6$	17.7
$10^3$	$910.5 \pm 78.8$	$755.2 \pm 99.4$	155.3
$10^4$	$1435.2 \pm 167.8$	$1267.4 \pm 143.2$	167.8
$10^5$	$1987.3 \pm 178.4$	$1699.2 \pm 155.8$	288.1
$10^6$	$2246.6 \pm 182.5$	$2054.5 \pm 247.4$	192.1

designed another set of experiments, which are given in the following paragraph.

In the new set of experiments time dependent tests were designed and applied in which  $10^6$  PFU  $\text{mL}^{-1}$  T4 phage and  $10^4$  CFU  $\text{mL}^{-1}$  *E. coli* K12 or *S. aureus* were used, as reported also in similar studies<sup>22,34</sup> (Fig. 5). It should be noted that the minimum exposure time was 10 min to ensure proper equilibration of the sensor device (for thermal equilibration and settling of the bacteria at the electrode surface). As shown in Fig. 5, there is an initial increase in the  $R_{ct}$  values, which is attributed to the arrival/adsorption of the intact target bacteria (*E. coli*) at the phage-modified electrode surface, and maximum values are reached in about 25–30 min. The  $R_{ct}$  sharply increased after the interaction of the target bacteria *E. coli* K12 with its specific T4 bacteriophage on the pencil electrodes for 20 min then it

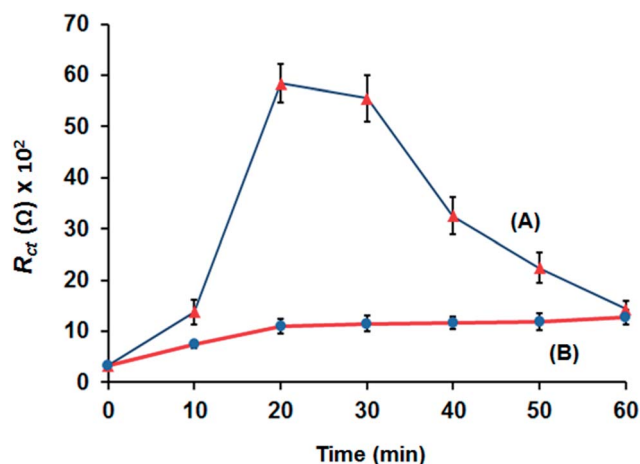


**Fig. 5** Changes in the  $R_{ct}$  values (average values  $\pm$  standard deviations) with time obtained with EIS, where the phage carrying PGEs (phages were adsorbed from the phage stock ( $100 \mu\text{L}$ ,  $10^6$  PFU  $\text{mL}^{-1}$ )) were incubated with bacterial suspensions containing  $10^4$  CFU  $\text{mL}^{-1}$  of the target bacteria, i.e., (A) *E. coli* and (B) *S. aureus* at room temperature.

decreased. This decrease is due to the infection of *E. coli* and lytic activity (results in the release of the bacterial cell content) which results in a significant reduction in the  $R_{ct}$  values. This behavior is also demonstrated visually in the SEM pictures given in Fig. 2. In contrast there was no significant change in the  $R_{ct}$  value in the presence of  $10^6$  CFU  $\text{mL}^{-1}$  *S. aureus*. From this result it may be concluded that T4-phages are specific for only *E. coli*. The gradual decrease observed for longer periods of time provide an indication that the infection of *E. coli* and the lytic cycle starts, which normally occurs within 20–35 min depending on the temperature.<sup>22,34</sup>

## Conclusion

In this study, low-cost (almost no cost) pencil graphite electrodes were used, and gold nanorods (GNRs) were deposited on them by a simple adsorption process. These electrodes work even at relatively low nanorod concentrations, which not only increase the sensitivity of the PGEs by increasing the surface conductance in EIS measurements but also helps to successfully immobilize the lytic phage T4 (by a simple self-assembling orientation) to act as a bio-probe for the detection of *E. coli* K12 cells. Impedance measurements performed with these electrodes provide a rapid, direct, and label-free means of detecting specific bacteria using a simple phage-based approach. Nyquist graphs were obtained and the surface charge transfer resistance,  $R_{ct}$ , values were calculated and used to demonstrate the results. These electrodes were used in the media containing different amounts of both target and non-target bacteria, specifically *E. coli* and *S. aureus* ( $100 \mu\text{L}$ ,  $10^2$  to  $10^6$  CFU  $\text{mL}^{-1}$ ). The minimum detection limit was approximately  $10^2$  CFU  $\text{mL}^{-1}$  in  $100 \mu\text{L}$  target suspension. In order to observe selectivity, the time dependent measurements of T4-phages and their target and non-target bacteria, *E. coli* and *S. aureus*, was performed. It is concluded that a 25–30 min test

period is enough to observe lytic activity which demonstrates the very specific detection of the target bacteria with their specific lytic phage. Additional important data was obtained with the non-target bacteria *S. aureus*, in which there is no time dependent change in the respective surface resistances after reaching a certain surface deposition. It seems that phages work well, even though the phages were immobilized *via* a simple adsorption protocol, which makes this detection methodology very attractive (simple and easy to apply). Most probably, the gold nanorods on the surfaces help the orientation of the phages immobilized by proper self-assembling on the PGE surfaces. We did not attempt to immobilize phages on gold nanorod surfaces covalently for simplicity, therefore it is not an over assumption that this approach works well. In contrast to earlier reports presenting the detection of *E. coli* using bacteriophage based analyzing systems,<sup>42–44</sup> the preparation of GNRs modified PGEs developed for detection of *E. coli* was herein easier, less time consuming and requiring less chemicals.

There have been several attempts to immobilize phages on surfaces covalently and in the oriented form (tails are free to interact) to increase the effectiveness of immobilized phages against their target bacteria.<sup>8,22,34</sup> Passivating agents, mainly albumin, are usually used to cover the area where there is no probe (phages here) to increase selectivity.<sup>8,22,34</sup> However, all these steps increase the complexity, cost, *etc.* for the preparation of the detection modules. In addition, it should be noted that it is quite difficult to create monolayers of passivating agent, such as albumin, on surfaces, since most probably they do interact with each other and form aggregates, which is usually not taken into consideration in these types of studies. However, most likely they increase the surface resistance in EIS measurements. Further, one could easily imagine that similar agglomerations of phages between each other occur on the electrode surfaces due to non-specific interactions. These aggregates may in turn cause an increase in the interfacial resistance and also may result in activity loss, since phages in aggregates cannot interact with their target bacteria properly/effectively. The scenario may be even more complex when these electrodes carrying phages do interact with their target bacteria on surfaces. It should be noted that bacteria are much bigger than phages and certainly much more than albumin (bacteria are in the  $\mu\text{m}$  size range; the phage size is about 200 nm long and 80–100 nm wide for T4, and albumin is approximately 15 nm  $\times$  15 nm  $\times$  3 nm), they do have hydrophilic/hydrophobic and positively/negatively charged regions (patches), and they carry several functional groups at different regions. All these regions (domains) are open for nonspecific interactions between each other and entities on the surfaces. These non-specific interactions and accumulations on the electrode surfaces or even in the detection medium may change the EIS readings due to changes in the respective corresponding resistances, which may result in loss of quality of the data obtained. Considering all these complexities, we attempted to use simple approaches in this study, and tried to exhibit both the performances and limitations of EIS testing.

## Acknowledgements

This study is partially supported by EU-FP7-IAPP Nanobacterphage-SERS and Biyomedtek/NanoBMT. E. Piskin and A. Erdem were supported as the members of Turkish Academy of Sciences (TUBA). Dr Filiz Sayar's contributions (developing the original recipe for GNRs synthesis) are greatly appreciated. The SEM micrographs were obtained at İYTE-MAM, Urla, İzmir with the contributions of Aysel Tomak and Aytac Gul – we greatly appreciated.

## References

- 1 P. Belgrader, W. Benett, D. Hadley, J. Richards, P. Stratton, R. Mariella and F. Milanovich Jr, *Science*, 1999, **284**, 449.
- 2 R. L. Edelstein, C. R. Tamanaha, P. E. Sheehan, M. M. Miller, D. R. Baselt, L. J. Whitman and R. J. Colton, *Biosens. Bioelectron.*, 2000, **14**, 805.
- 3 J. Gau, E. H. Lan, B. Dunn, C. M. Ho and J. C. S. Woo, *Biosens. Bioelectron.*, 2001, **16**, 745.
- 4 E. A. Mothershed and A. M. Whitney, *Clin. Chim. Acta*, 2006, **363**, 206.
- 5 B. Byrne, E. Stack, N. Gilmartin and R. O'Kennedy, *Sensors*, 2009, **9**, 4407.
- 6 F. Farabullini, F. Lucarelli, I. Palchetti, G. Marrazza and M. Mascini, *Biosens. Bioelectron.*, 2007, **22**, 1544.
- 7 S. Balasubramanian, I. B. Sorokulova, V. J. Vodyanoy and A. L. Simonian, *Biosens. Bioelectron.*, 2007, **22**, 948.
- 8 A. Singh, S. Poshtiban and S. Evoy, *Sensors*, 2013, **13**, 1763.
- 9 V. Dharuman, T. Grunwald, E. Nebling, J. Albers, L. Blohm and R. Hintsch, *Biosens. Bioelectron.*, 2005, **21**, 645.
- 10 H. Huang, C. He, H. Zeng, X. Xi, X. Yu, P. Yi and Z. Chen, *Biosens. Bioelectron.*, 2009, **24**, 2255.
- 11 H. Huang, S. Huang, X. Liu, Y. Zeng, X. Yu, B. Liao and Y. Chen, *Biosens. Bioelectron.*, 2009, **24**, 3025.
- 12 A. Erdem, F. Sayar, H. Karadeniz, G. Guven, M. Ozsoz and E. Piskin, *Electroanalysis*, 2007, **19**, 798.
- 13 G. Congur, F. Sayar, A. Erdem and E. Piskin, *Colloids Surf., B*, 2013, **112**, 61.
- 14 J. S. Daniels and N. Pourmand, *Electroanalysis*, 2007, **19**, 1239.
- 15 O. Panke, T. Balkenhohl, J. Kafka, D. Schafer and F. Lisdat, *Adv. Biochem. Eng./Biotechnol.*, 2008, **109**, 195.
- 16 C. Ruan, L. Yang and Y. Li, *Anal. Chem.*, 2002, **74**, 4814.
- 17 S. M. Radke and E. C. Alcocilja, *IEEE Sens. J.*, 2005, **5**, 744.
- 18 G. Kim, J. H. Mun and A. S. Om, *J. Phys.: Conf. Ser.*, 2007, **61**, 555.
- 19 M. Varshney, Y. Li, B. Srinivasan and S. Tung, *Sens. Actuators, B*, 2007, **128**, 99.
- 20 O. Laczka, E. Baldrich, F. J. del Campo and F. X. Munoz, *Anal. Bioanal. Chem.*, 2008, **391**, 2825.
- 21 X. Munoz-Berbel, N. Godino, O. Laczka, E. Baldrich, F. X. Munoz and F. J. del Campo, in *Principles of Bacterial Detection: Biosensors, Recognition Receptors and Microsystems*, ed. M. Zourob, S. Elwary and A. Turner, Springer, 2008, vol. 15, pp. 339–374.
- 22 M. Shabani, B. Zouro, C. A. Allain, M. F. Marquette, R. Lawrence and R. Mandeville, *Anal. Chem.*, 2008, **80**, 9475.

- 23 R. D. Das, C. RoyChaudhuri, S. Maji, S. Das and H. Saha, *Biosens. Bioelectron.*, 2009, **24**, 3215.
- 24 M. Varshney and Y. B. Li, *Biosens. Bioelectron.*, 2009, **24**, 2951.
- 25 F. Sayar, (supervisor: E. Piskin), Production of Nanoparticles and Their Applications in Nanomedicine, PhD thesis, Hacettepe University, Chemical Engineering Department and Bioengineering Division, Turkey, 2010.
- 26 L. T. Lanh, T. T. Hoa, N. C. Cuong, D. Q. Khieu, D. T. Quang, N. Van Duy, N. C. Hoa and N. V. Hieu, *J. Alloys Compd.*, 2015, **635**, 265.
- 27 X. Ma, M. C. Wang, J. Feng and X. Zhao, *J. Alloys Compd.*, 2015, **637**, 36.
- 28 H. Huang, C. Tang, Y. Zeng, X. Yu, B. Liao, X. Xia, P. Yi and P. K. Chu, *Colloids Surf., B*, 2009, **71**, 96.
- 29 Z. Ma, L. Tian, T. Wang and C. Wang, *Anal. Chim. Acta*, 2010, **673**, 179.
- 30 B. Pan, D. Cui, P. Xu, Q. Li, T. Huang, R. He and F. Gao, *Colloids Surf., A*, 2007, **295**, 217.
- 31 C. Z. Li, K. B. Male, S. Hrapovic and J. H. T. Luong, *Chem. Commun.*, 2005, 3924.
- 32 Y. H. Won, K. Huh and L. A. Stanciu, *Biosens. Bioelectron.*, 2011, **26**, 4514.
- 33 J. Sambrook and D. W. Russell, *Molecular Cloning: A Laboratory Manual*, Cold Spring Harbor Laboratory Press, New York, 2nd edn, 1989.
- 34 M. B. Mejri, H. Baccar, E. Baldrich, F. J. Del Campo, S. Helali, T. Ktari, A. Simonian, M. Aouni and A. Abdelghani, *Biosens. Bioelectron.*, 2010, **26**, 1261.
- 35 M. Abdul Aziz and A. N. Kawde, *Talanta*, 2013, **115**, 214.
- 36 J. Gao, C. M. Bender and C. Murphy, *Langmuir*, 2003, **19**, 9065.
- 37 Q. Dai, J. Coutts, J. Zou and Q. Huo, *Chem. Commun.*, 2008, 2858.
- 38 N. R. Jana, C. J. Gearheart and C. Murphy, *Chem. Mater.*, 2001, **13**, 2313.
- 39 S. J. Lee, V. Anandan and G. Zhang, *Biosens. Bioelectron.*, 2008, **23**, 1117.
- 40 V. Dharuman, T. Grunwald, E. Nebling, J. Albers, L. Blohm and R. Hintsch, *Biosens. Bioelectron.*, 2005, **21**, 645.
- 41 X. Munoz-Berbel, N. Godino, O. Laczka, E. Baldrich, F. X. Munoz and F. J. del Campo, in *Principles of Bacterial Detection: Biosensors, Recognition Receptors and Microsystems*, ed. M. Zourob, S. Elwary and A. Turner, Springer, 2008, vol. 15, pp. 339–374.
- 42 M. SoonCheng, J. S. Ho, S. H. Lau, V. T. K. Chowb and C. S. Toh, *Biosens. Bioelectron.*, 2013, **47**, 340.
- 43 A. Shabani, C. A. Marquette, R. Mandeville and M. F. Lawrence, *Talanta*, 2013, **116**, 1047.
- 44 B. Prieto-Simón, N. M. Bandaru, C. Saint and N. M. Voelcker, *Biosens. Bioelectron.*, 2015, **67**, 642.